Metabolomics Reveals the Renoprotective Effect of N-butanol Extract and Amygdalin Extract From Amygdalus Mongolica in Rats With Renal Fibrosis

wanfu BAI
Baotou Medical College
Qing Liu
Baotou Medical College
Hong Chang
Baotou Medical College
Quanli Liu
Baotou Medical College
Chen Gao
Baotou Medical College
Yingchun Bai
Baotou Medical College
Hongbing Zhou
Baotou Medical College
Songli Shi (shisongli122@126.com)
Baotou Medical College

Research

Keywords: serum metabolomics, renal fibrosis, Amygdalus mongolica, protective effect, n-butanol extract, amygdalin extract

DOI: https://doi.org/10.21203/rs.3.rs-74776/v1

Abstract

Background: Renal fibrosis is a pathological process of progression from chronic kidney disease to end-stage renal disease, which threaten human health. *Amygdalus mongolica* is a traditional Chinese medicine, and our previous studies demonstrated that the n-butanol extract (BUT) and amygdalin extract (AMY) from its seeds, which are effective components of *A. mongolica,* can prevent renal fibrosis (RF). The present study was to investigate the exact mechanism of the protective effect of *A. mongolica* on RF.

Methods: The RF rat model was established through unilateral ureteral obstruction (UUO). Biochemical indicators were measured, combined with histopathology of renal tissue, to evaluate the anti-RF effects of the extracts of *A. mongolica*. A serum metabonomic method based on UPLC-QTOF-MS was used to clarify the changes in the metabolic profile among the different groups.

Results: We found that tubulointerstitial damage and fibrosis were significantly improved, metabolic perturbations were restored after treatment with BUT and AMY. Thirty-eight metabolites associated with RF progression and related to the regulation of arginine and proline metabolism, nicotinate and nicotinamide metabolism, histidine metabolism and pentose and glucuronate interconversions were identified. They were restored to levels similar to those observed in controls by treatment with AMY and BUT. Moreover, no significant differences in efficacy were observed between the BUT and AMY groups.

Conclusions: The results demonstrated that antifibrotic effects of *A. mongolica* in rats with RF. It was the first to reveal the potential mechanisms of the renoprotective effects after treatment with BUT and AMY from *A. mongolica*.

Background

Renal fibrosis (RF) is a pathological injury process that can lead to continuous deterioration in various chronic renal diseases until the gradual loss of kidney function due to wound infection, inflammation, blood circulation obstacles, and various pathogenic factors stimulates the immune response. RF progressively induces cell damage, develops late in life, results in marked collagen deposition and accumulation, and causes sclerosis of the renal parenchyma and scarring until the kidneys completely lose visceral function. Moreover, RF causes cellular hardening and induces abnormal extracellular matrix (ECM) deposition [1].

Amygdalus mongolica (Maxim.) Ricker from the Rosaceae family is a special medicinal material in Inner Mongolia. The seeds of *A. mongolica* are used as a traditional herbal medicine [2, 3]. The amygdalin monomer was obtained from the n-butanol extract (BUT) of *A. mongolica*. We previously identified amygdalin as the main bioactive compound and found that it accounted for 47.72% of the content of BUT. The molecular formula of amygdalin is $C_{20}H_{27}NO_{11}$. Because it is an organic compound containing nitrogen atoms, amygdalin is also an alkaloid compound [4]. In a previous study, we demonstrated that *A. mongolica* extract has protective effects on the liver fibrosis induced by carbon tetrachloride in rats [3]. The present study aimed to observe the therapeutic effect and mechanism of *A. mongolica* extract on rats with RF and to provide a scientific basis for finding effective drugs against liver fibrosis. Emodin and amygdalin are the main biologically active components of *A. mongolica* [4]. Other studies have shown that amygdalin exhibits antifibrogenic effects in the liver and renal [3-8]. Therefore, the study of these ingredients will help us to understand the antifibrotic mechanism of *A. mongolica*. However, because of the complex interactions among the active ingredients, little is known about the exact mechanism by which *A. mongolica* prevents RF. Therefore, we focused on the effects of the Amygdalin monomer and the n-butanol extract in the process of RF.

Moreover, new methods are urgently needed to elucidate these complex mechanisms to find effective anti-RF drugs and to comprehensively evaluate the systematic clinical efficacy of *A. mongolica*. Metabolomics uses animal fluids, tissues and cells as research objects and monitors the dynamic changes in metabolite composition, quality and quantity induced by

physiological, pathological or drug stimulation. Metabolomics analyzes the whole spectrum of low molecular weight compounds, rather than focusing on individual metabolites. Moreover, metabolomics approaches produces a generic framework that provides information on the functional integrity of the entire organism in a stage of a disease or after a given intervention [9]. Therefore, metabolomics, as an analytical platform, can be used to discover novel biomarkers involved in different disease processes [10] and to evaluate drug efficacy [11] and safety [12]. Among the metabolomics analysis tools, UPLC-QTOF-MS has become useful because of its good separation efficiency and detection sensitivity [13]. We used this method to explore the possible antifibrotic mechanisms of *A. mongolica*. The experiment was carried out according to the flow design shown in Fig. 1.

Materials And Methods

Chemicals

Seeds of *Amygdalus mongolica* were obtained from Alashan in Inner Mongolia. Professor Songli Shi of Inner Mongolia University of Science and Technology Medical College of Baotou identified dried mature seeds. Carboxymethylcellulose sodium and pentobarbital sodium were purchased from Tianjin Kaitong Chemical Reagent Co., Ltd. and Merck Germany Ltd., respectively. The purity of these chemicals (analytical grade) was above 99.5% (Tianjin, China). An MDA kit, superoxide dismutase (SOD) kit, hydroxyproline (HYP) kit, quantitative determination kit for total protein, and Masson staining kit were purchased from Nanjing Jiancheng Bioengineering Institute (Nanjing, China). HPLC-grade methanol, acetonitrile and formic acid were purchased from Honeywell (USA).

Preparation and Analysis of A. mongolica Extracts

The seeds of *A. mongolica* were peeled to remove the seed shells and crushed. Solutions of 95% and 70% ethanol were used as the extraction solvents. The conditions of the extraction were as follows: temperature, 70°C; solid-liquid ratio, 1:10; and time, 2 hr. The combined extracts were concentrated under pressure to obtain a brown ethanol extract. The ethanol extract was partitioned with water and three organic solvents with different polarities (petroleum ether (PE) < ethyl acetate (EA) < n-butanol (BU)) to obtain the PE extract, EA extract, and BUT, respectively. After concentration and drying, BUT was obtained. The isolation and identification of amygdalin from BUT of *A. mongolica* were described in previous studies [14]. Amygdalin was derived from BUT and accounted for 47.72% of BUT content.

Analysis of BUT and isolation and identification of amygdalin

TLC spray reagents containing bismuth potassium iodide indicated the presence of alkaloids. The BUT of *A. mongolica* was added to D101 macroporous resin column by the wet method and eluted with 10%, 30%, 50%, 70%, and 90% ethanol, respectively. The flow component was detected by thin-layer silica gel chromatography. The developing solvent was carbon tetrachloride:methanol (4:1). The 10% and 30% ethanol eluents were added to ODS column by the wet method and eluted with methanol solution. The developing solvent was ethyl acetate:formic acid:water (20:3:1). According to the TLC results, the liquid components with the same chromatographic characteristics were combined, the solvent was recovered, and a colorless powder was obtained. The powder was then identified by UPLC□DAD□ESI□MS and nuclear magnetic resonance analysis. Chromatographic conditions: The chromatographic column was Agilent ZORBAX Eclipse Plus C_{18} (2.1mm × 50mm), particle size, 1.8 μm). Mobile phase A was 0.1% formic acid solution, mobile phase B was methanol, and the flow rate was 0.4 mL/min. The elution gradient was as follows: 0 - 3 min 10% - 30% B, 4 - 5 min 30% - 100% B, 5 - 6 min 100% B. With D_2O as the solvent, the NMR spectra of the isolated compounds were obtained at a frequency of 500 MHZ. The result showed that the compound was amygdalin (Fig. S1).

Animals and sample collection

The animal experiments were approved by the Ethical Committee of Baotou Medical College (Approval Number: 20190314). Male Sprague-Dawley rats (purchased from animal Experiment Center of Peking University Health Science Center, number of animal license SCXK 2017-0005) were randomly divided into the control (CON) group (n = 8), model (MOD) group (n = 8), BUT group (n = 8) and amygdalin extract (AMY) group (n = 8). Rats in the MOD, BUT and AMY groups underwent unilateral ureteral obstruction (UUO) to establish a model of RF. The UUO method are described in Supplementary information. Only the left ureter was separated and ligated, and the abdominal cavity was closed in the sham operation group. The BUT and AMY groups were gastrically administered BUT (1.25 g•kg/d) and AMY (0.02 g•kg/d), respectively, for 3 weeks. An equal volume (4 mL•kg/d) of saline was administered to the rats in the CON and MOD groups. The general condition of the rats was observed, the number of deaths was recorded, and rats were allowed to drink and eat freely. The laboratory temperature was 21 °C - 27 °C, and the relative humidity was 30 °C - 50 °C.

Blood was obtained from the abdominal aorta of rats after anesthetization with pentobarbital (35 mg/kg of bodyweight) (Merck Ltd., Germany). Serum was obtained from blood samples by centrifugation and stored at −80 °C. Tissues from the left kidney were fixed with 10% paraformaldehyde, and pathological changes were observed in paraffin sections.

Histological Changes

The paraffin-embedded kidney tissues were cut into 5-μm sections, and hematoxylin & eosin (H&E) and Masson staining were performed to observe pathological changes [15]. The score of fibrosis injury was determined according to the description by Zhi-Hao Zhang [16, 17] in ten randomly selected nonoverlapping fields per rat.

Biochemical Indicator Measurements

Blood was centrifuged at 3000 rpm for 15 minutes, and serum was removed and detected by an automatic biochemical instrument. Biochemical parameters were measured using an Olympus AU640 automatic analyzer (Olympus, Japan) [17].

Serum sample preparation and UPLC–QTOF-MS assay

All serum samples were thawed in an ice water bath and vortex-mixed before analysis. The analysis of six random serum samples in each group by UPLC-QTOF-MS is detailed in the Supplementary Information (Chang et al. 2017).

Serum Metabolomics Study and Data Analysis

The blood metabolic profiles of the rats were imported into MarkerLynx software for data reduction and to acquire mass spectrometry matrix information. The EZinfo software module was then used to conduct principal component analysis (PCA) with the data in each group, and the differences in the metabolic profiles of each group were identified.

To more effectively identify differences in metabolites, the blood metabolic profile of each group of rats was further analyzed by partial least square discriminant analysis (PLS-DA) [18], and a VIP plot was obtained that showed the metabolic differences among the groups. P-values were obtained from the VIP plot and two-tailed Student's t-test. HMDB KEGG, MetPA and other data platforms were used to retrieve potential biomarkers [13, 19].

Results

Histological Changes

Micrographs of renal tissue with H&E staining and Masson staining showed that the renal tubules in the CON group remained intact and that the interstitium did not significantly change (Fig. 2 (a, e)). In the MOD group, inflammatory cells infiltrated, renal tubules atrophied, and interstitial fibrosis was observed. Masson staining showed vacuolar changes in renal tubular epithelial cells and ECM deposition with fibrosis (Fig. 1 (b, f)). Inflammation and fibrosis were improved in the MOD group after the administration of AMY and BUT (Fig. 2 (c, d, g, h)). The histopathological score showed the extent of damage to the tissues (Fig. 2i). The results showed that the BUT and AMY from *A. mongolica* had certain protective effects on RF in rats.

Determination of Clinical Biomarkers of Renal Function

Biochemical markers associated with renal function in clinical settings, including blood diabetic nitrogen (BUN), serum creatinine (Scr), HYP (routine markers of fibrosis) and antioxidant index, were detected in the MOD, CON, BUT and AMY groups. The levels of Scr, HYP, albumin (ALB), BUN and malondialdehyde (MDA) were increased in the model group compared with the CON group ($p < 0.05$ or $p < 0.01$). The level of SOD was decreased ($p < 0.05$ or $p < 0.01$) in the MOD group compared with the CON group (shown in Fig. 2j and Table S1). After treatment with BUT and AMY, biochemical indicators related to renal function tended to be restored to normal levels. The anti-RF effects of *A. mongolica* were shown through the changes in the biochemical markers above.

Comparison of Different Groups Using PCA and PLS-DA

The metabolic profiles of serum samples from different groups were determined by UPLC-QTOF-MS in the positive and negative electrospray ionization (ESI) modes. According to the PCA results, the CON and MOD groups were divided into two areas, as shown in the PCA score plot (Fig. 3 (a, b)). This result suggested that we successfully established the UUO model. Furthermore, the AMY and BUT groups were clearly separated from the MOD group. PLS-DA was used to maximize differences in metabolic profiles (Fig. 3 (e, f)), which were verified by class permutation tests (shown in Fig. 3 (g, h)). The R^2 and Q^2 values were 0.82 and 0.28, respectively, in the positive mode, and the R^2 and Q^2 values were 0.79 and 0.36, respectively, in the negative mode. The values indicate that these models have good fitness and prediction.

Screening and Identification of Metabolic Differences

We identified thirty-eight differentially expressed metabolites between the CON and MOD groups based on VIP > 2 and $P < 0.05$, which provided more rigorous screening than VIP > 1 and $P < 0.05$ in the V-plots (Fig. 3 (c, d)). In order to verify the diagnostic potential of 38 potential biomarkers, ROC analysis was performed, and the results showed that the AUC value of all 38 potential biomarkers was above 0.9 (Fig. 3 (i, j, k, l)), indicating that these metabolites had good stability. Among these differentially expressed metabolites, 22 metabolites were identified in the positive ion mode, 10 of which were upregulated and 12 of which were downregulated. In the negative ion mode, 16 metabolites were identified, 8 of which were upregulated and 8 of which were downregulated (as listed in Table 1). The thirty-eight metabolites can be divided into 7 classes, including 2 benzenoids, 4 lipids and lipid-like molecules, 4 nucleosides, nucleotides, and analogs, 13 organic acids and derivatives, 8 organic oxygen compounds, 6 organoheterocyclic compounds, 1 organic nitrogen compound (Fig. 4a). These results are shown in a heat map showing relative increases (red) or decreases (green) in the MOD group compared with the CON group. Many of these metabolites were reversed after treatment with BUT and AMY (Fig. 4c).

Metabolic Pathway and Protective Effects of Amygdalus mongolica Analysis

To directly measure the correlations between the 38 metabolites, Pearson rank correlation analysis (Fig. 5a) was performed. The Pearson correlation coefficients of 32 metabolites were $r > 0.8$ and $r \leq -0.8$. The results showed that they are potential biomarkers. These significantly expressed metabolites were subjected to MetPA pathway enrichment and functional analysis, and the results showed that the metabolites are involved in metabolic pathways (Fig. 5b), including nicotinate and nicotinamide metabolism, pentose and glucuronate interconversions, arginine and proline metabolism, arginine biosynthesis, histidine metabolism, cysteine and methionine metabolism, and amino sugar and nucleotide sugar metabolism. These pathways may be related to the occurrence of RF.

In addition, in the AMY group compared with the MOD group, 48 metabolites were selected and identified (VIP > 2 and $P < 0.05$), of which the concentrations of 47 metabolites were reversed or returned to normal levels (Fig. S2 (a, b), Table S2). In the BUT group compared with the MOD group, 53 metabolites were identified (VIP > 2 and $P < 0.05$), of which the concentrations of 48 were reversed (Fig. S2 (c, d), Table S3). BUT and AMY from *A. mongolica* may exert protective effects on rats with RF by acting on the above metabolic pathways.

To reveal changes in metabolites and the mechanism of fibrosis treatment with BUT and AMY, the differential metabolites were analyzed by KEGG enrichment. Among the 38 differentially expressed metabolites between the CON and MOD groups, 18 metabolites were acted on by either BUT or AMY, and 14 metabolites were co-acted on by BUT and AMY (Fig. 4b, Table 1). The KEGG enrichment results showed that the metabolic pathways of nicotinate and nicotinamide metabolism, histidine metabolism, and purine metabolism were significantly changed in the BUT and AMY groups. These pathways are associated with oxidative stress, the release of inflammatory cytokines and pro-fibrogenic factors, which can promote fibrinolysis. In addition, AMY can also act on pentose and glucuronate interconversions, which was significantly enriched and associated with improving body energy metabolism (Fig. 5c).

Discussion

RF is usually an insidious progression of chronic kidney disease (CKD), and the initial symptoms are not obvious. Biomarkers can be used not only as specific diagnostic tools but also as therapeutic targets for diseases. In this study, through metabolomics analysis, nicotinate and nicotinamide metabolism, pentose and glucuronate interconversions, arginine and proline metabolism, arginine biosynthesis, histidine metabolism, cysteine and methionine metabolism and amino sugar and nucleotide sugar metabolism were found to be related to RF. Therefore, because of their involvement in the development of RF, these metabolic pathways and metabolites could be used to accurately diagnose early RF and as targets to reverse CKD [20].

Unilateral ureteral ligation is widely used in animal models for pharmacology studies. Ligating the renal drainage system in UUO can cause changes in acute renal function and chronic damage to the kidney because it increases urinary pressure, decreases renal blood flow, and promotes venous blockage, macrophage infiltration, and fiber cell proliferation; thus, UUO gradually develops into renal interstitial fibrosis [21].

Among the 38 differentially expressed metabolites between the CON and MOD groups, 18 metabolites were acted on by either BUT or AMY, and 14 metabolites were co-acted on by BUT and AMY. Four metabolites were acted on by BUT alone. For example, diketogulonic acid (DKG) may be involved in damage to the kidney caused by oxalate. DKG is a metabolite of the degradation of vitamin C. The degradation pathway of vitamin C produces L-erythrulose and oxalate as final products, and the oxalate formed in this way may contribute to the formation of kidney stones in susceptible individuals. AMY alone acts on 4 metabolites, which increase the excretion of toxic substances by increasing the conjugation of glucuronic acids. Glucuronidation assist the excretion of toxic substances, drugs, and other substances that cannot be used as an energy source.

Ornithine can improve athletic performance through anabolic and wound healing effects, and it can enhance immune function in cells. L-Ornithine is located in the mitochondria and cytoplasm. Moreover, ornithine is associated with cystinuria,

hyperdibasic aminoaciduria, and lysinuric protein intolerance, which are genetic metabolic defects. Ornithine is produced in the urea cycle through the cleavage of urea from arginine [20]. L-Ornithine is also a precursor of proline, citrulline and arginine. Proline is the elementary element of collagen tissue and can promote collagen synthesis and deposition at the lesion site.

Hydroxyproline is one of the main components of collagen and is unique to collagen fibers. The content of hydroxyproline in renal tissue is closely related to the severity of renal interstitial fibrosis. Therefore, hydroxyproline content can be an indicator to judge the severity of renal interstitial fibrosis.

S-adenosine homocysteine (SAH) is the demethylation product of S-adenosylmethionine (SAM), and SAH hydrolyzed into adenosine (Ado). Ado primarily regulates most of internal organ function. SAM is a major methyl donor, and increasing concentrations of this molecule indicate RF and subsequent impaired kidney function.

Homocysteine (Hcy) is a sulfur-containing amino acid and is an important intermediate product of methionine metabolism [13, 22]. Hcy leads to impaired renal function, which is mainly related to oxidative stress, endoplasmic reticulum stress and four other aspects [23]. Meyrier et al. [24] found that increased Hcy levels can lead to glomerular sclerosis, renal tubular atrophy, interstitial fibrosis and a decreased glomerular filtration rate. Hiromichi et al. [25] and Li et al. [26] found arterial and arteriolar wall thickening and focal tubular interstitial fibrosis in the kidneys of rats with high Hcy and suggested that increased plasma Hcy may be an important pathogenic factor for glomerular injury in hypertension.

We also compared the changes in metabolomics induced by BUT and AMY in the treatment of RF. Nicotinate and nicotinamide metabolism, histidine metabolism and purine metabolism were influenced by both BUT and AMY. We found that AMY also regulates the disruption of pentose and glucuronate interconversions, nicotinate and bile secretion [27]. Thus, these pathways were probably the main metabolic pathways involved in the therapeutic effect of the active ingredients in BUT [28].

The main difference in metabolomics between the BUT and AMY groups is that pentose and glucuronate interconversions were more significantly impacted by AMY, which suggests that amygdalin from *A. mongolica* improves metabolic disorders caused by fibrosis mainly by acting on both pathways. Notably, amygdalin has a significant regulatory effect on SAM, and indoxyl glucuronide. Based on the above speculation, we will conduct more in-depth verification and discussion in future research.

Conclusion

In summary, through this serum metabolomics study based on UPLC-QTOF-MS, we found that BUT and AMY from *A. mongolica* could improve the changes in the metabolic profile of blood caused by fibrosis. Both had protective effects on rats with renal fibrosis. In addition, amygdalin regulates disrupted pentose and glucuronate interconversions, consequently blocking the progression of fibrosis. In the present study, some potential biomarkers in the development of RF were identified, and the mechanism of BUT and AMY in the treatment of RF was revealed from the perspective of metabolic pathways. In the future, we will verify the metabolic characteristics of this study using human samples.

Abbreviations

BUT, n-butanol extract; AMY, amygdalin extract; RF, renal fibrosis; PCA, principal component analysis; PLS-DA, partial least square discriminant analysis; UPLC-QTOF-MS, ultra performance liquid chromatography-quadrupole time of flight-mass spectrometry; ECM, extracellular matrix; SOD, superoxide dismutase; HYP, hydroxyproline; PE, petroleum ether; EA, ethyl acetate; BU, n-butanol; MDA, malondialdehyde; HPLC, high performance liquid chromatography; CON, control; MOD, model; H&E, hematoxylin & eosin; HMDB, human metabolome database; KEGG, Kyoto Encyclopedia of Genes and Genomes; BUN, blood diabetic nitrogen; Scr, serum creatinine; ALB, albumin; CKD, chronic kidney disease; DKG, Diketogulonic acid; SAH, S-

adenosine homocysteine; SAM, S-adenosylmethioninamine; Ado, adenosine; Hcy, Homocysteine; UUO, unilateral ureteral obstruction.

Declarations

Acknowledgements

The authors thank the help of LC-BIO TECHNOLOGIES (HANGZHOU) CO., LTD.

Authors' contributions

Wan-fu Bai carried out the experiments, participated in the study design and wrote the paper. Chen Gao and Ying-chun Bai completed model with unilateral ureteral obstruction. Qing Liu completed and analyzed the extract. Hong Chang completed the pathological section and analysis. Hong-bing Zhou and Quan-li Liu were involved in the anti-oxidant activity test in rats. Song-li Shi guided all experiments and revised the article.

Funding

This research was financially supported by the National Natural Science Foundation of China (NSFC) [No. 81641137 and No. 81760782]; the Natural Science Foundation of Inner Mongolia Autonomous Region of China [No. 2018LH03027 and No. 2019MS08189]; a Scientific Research Fund Project of Baotou Medical College [No. BYJJ-YF 201706]; a Baotou Medical College Doctoral Scientific Research Foundation Project [No.BSJJ201814]; and a Grassland Talent Project [No. Q2017046].

Availability of data and materials

The datasets used and/or analyzed during the current study are available from the corresponding author on reasonable request.

Ethics approval and consent to participate

The animal experiments were approved by the Ethical Committee of Baotou Medical College (Approval Number: 20190314).

Consent for publication

Not applicable.

Competing interests

The authors declare that they have no competing interests.

References

1. Sonja D, Peter B. Cellular and molecular mechanisms of kidney fibrosis. Mol Aspects Med. 2018;65:16-36.

2. Yang G, Xu G. Study on the Analysis of Yuliren by TLC and Electrophoresis. Journal of China Pharmaceutical University. 1992;2(2):77-81.
3. Wu T, Chang H, Shi S, Zhou H, Wu P, Zheng Q, et al. Effect of Petroleum Ether Extracts of Amygdalus mongolica on Liver Fibrosis Rat Models Induced by Carbon Tetrachloride. Chinese Archives of Traditional Chinese Medicine. 2017;35:595-598.
4. Zheng QN, Wang J, Zhou HB, Niu SF, Liu QL, Yang ZJ, et al. Effectiveness of Amygdalus mongolica oil in hyperlipidemic rats and underlying antioxidant processes. J Toxicol Environ Health A. 2017;80(22):1193-1198. https://doi: 10.1080/15287394.2017.1367124
5. Sun L, Yuan XL, Sun LD, Zhao XN. The effect and significance of emodin on expression of tissue inhibitor of platelet derived growth factors-B (PDGF-B) in rat with renal tubulointer-stitial fibrosis. Chinese Journal of Birth Health & Heredity. 2016;24:29-30.
6. ShuLan C, XuDong D, JinAo G, Sheng C, HongDie T. Renal protective effect and action mechanism of Huangkui capsule and its main five flavonoids. Journal of Ethnopharmacology An Interdisciplinary Journal Devoted to Bioscientific Research on Indigenous Drugs. 2017;206:152-159.
7. Chen SL, Guang-Li DU, Ding N, Jin HX, Chen DX. Comparative Study of Xiayuxue Decoction and Its Ingredients Recipe Against Porcine Serum Induced Liver Fibrosis in Rats. Chinese Journal of Experimental Traditional Medical Formulae. 2012;18:154-157.
8. Shao-li C, Guang-li D, Yan-ping L, Yan-yan T, De-xing C. Effect of "Xiayuxue Decoction" and Componential Prescription on Expressions of COL-Iα1 and TIMP-1 mRNA in Rats with Immunologic Hepatic Fibrosis:A Comparative Study. Acta Universitatis Traditionis Medicalis Sinensis Pharmacologiaeque Shanghai. 2012;26:82-85.
9. Cai S, Huo T, Xu J, Lu X, Zheng S, Li F. Effect of mitiglinide on Streptozotocin-induced experimental type 2 diabetic rats: a urinary metabonomics study based on ultra-performance liquid chromatography-tandem mass spectrometry. Journal of Chromatography B Analytical Technologies in the Biomedical & Life Ences. 2009;877(29):3619-3624.
10. Yang J, Xu G, Zheng Y, Kong H, Pang T, Lv S, et al. Diagnosis of liver cancer using HPLC-based metabonomics avoiding false-positive result from hepatitis and hepatocirrhosis diseases. Journal of Chromatography B. 2004;813(1-2):59-65.
11. Zhao X, Zhang Y, Meng X, Yin P, Deng C, Chen J, et al. Effect of a traditional Chinese medicine preparation Xindi soft capsule on rat model of acute blood stasis: a urinary metabonomics study based on liquid chromatography-mass spectrometry. J Chromatogr B Analyt Technol Biomed Life Sci. 2008;873(2):151-158. doi: 10.1016/j.jchromb.2008.08.010
12. Ma C, Bi K, Zhang M, Su D, Fan X, Ji W, et al. Toxicology effects of Morning Glory Seed in rat: A metabonomic method for profiling of urine metabolic changes. J Ethnopharmacol. 2010;130(1):134-142.
13. Chang H, Meng HY, Liu SM, Wang Y, Yang XX, Lu F, et al. Identification of key metabolic changes during liver fibrosis progression in rats using a urine and serum metabolomics approach. Scientific Reports. 2017;7(1):11433.
14. Zhao YS, Pei-Sai WU, Zhang HW, Cheng XH, Shi SL, Liu QL, et al. Studies on dose-effect relationship of n-butanol extracts of Amygdalus mongolica on reducing blood lipid and its chemical constituents. Ence & Technology of Food Industry. 2017;38:348-352.
15. Ya BL, Li HF, Wang HY, Wu F, Ge F. 5-HMF attenuates striatum oxidative damage via Nrf2/ARE signaling pathway following transient global cerebral ischemia. Cell Stress Chaperones. 2016;22(1):1-11.
16. Zhang ZH, Li MH, Liu D, Chen H, Chen DQ, Tan NH, et al. Rhubarb Protect Against Tubulointerstitial Fibrosis by Inhibiting TGF-beta/Smad Pathway and Improving Abnormal Metabolome in Chronic Kidney Disease. Front Pharmacol. 2018;9:1029. doi: 10.3389/fphar.2018.01029
17. Zhang ZH, Vaziri ND, Wei F, Cheng XL, Bai X, Zhao YY. An integrated lipidomics and metabolomics reveal nephroprotective effect and biochemical mechanism of Rheum officinale in chronic renal failure. Sci Rep. 2016;6:22151. doi: 10.1038/srep22151

18. Jung S, Song SW, Lee S, Kim SH, Ann SJ, Cheon EJ, et al. Metabolic phenotyping of human atherosclerotic plaques: Metabolic alterations and their biological relevance in plaque-containing aorta. Atherosclerosis. 2018;269:21-28.
19. Fang J, Wang W, Sun S, Wang Y, Li Q, Lu X, et al. Metabolomics study of renal fibrosis and intervention effects of total aglycone extracts of Scutellaria baicalensis in unilateral ureteral obstruction rats. J Ethnopharmacol. 2016;192:20-29.
20. Morizono H, Woolston JE, Colombini M, Tuchman M. The use of yeast mitochondria to study the properties of wild-type and mutant human mitochondrial ornithine transporter. Molecular Genetics & Metabolism. 2005;86(4):431-440.
21. Zhao L, Dong M, Liao S, Du Y, Zhou Q, Zheng H, et al. Identification of key metabolic changes in renal interstitial fibrosis rats using metabonomics and pharmacology. Sci Rep. 2016;6:27194. doi: 10.1038/srep27194
22. Li A, Shi Y, Xu L, Zhang Y, Zhao H, Li Q, et al. A possible synergistic effect of MTHFR C677T polymorphism on homocysteine level variations increased risk for ischemic stroke. Medicine. 2017;96(51):e9300.
23. Yi F, Li PL. Mechanisms of homocysteine-induced glomerular injury and sclerosis. Am J Nephrol. 2008;28(2):254-264. doi: 10.1159/000110876
24. Meyrier A, Hill GS, Simon P. Ischemic renal diseases: New insights into old entities. Kidney Int. 1998;54(1):2-13.
25. Kumagai H, Katoh S, Hirosawa K, Kimura M, Hishida A, Ikegaya N. Renal tubulointerstitial injury in weanling rats with hyperhomocysteinemia. 2002;62:1219-1228.
26. Li N, Chen YF, Zou AP. Implications of Hyperhomocysteinemia in Glomerular Sclerosis in Hypertension. Hypertension. 2002;39(2):443.
27. Vital-Lopez FG, Jaques R, Anders W, Maranas CD. Biofilm Formation Mechanisms of Pseudomonas aeruginosa Predicted via Genome-Scale Kinetic Models of Bacterial Metabolism. PLoS Comp Biol. 2015;11(10):e1004452.
28. Hong C, Qing L, AWan Fu B, Ying Chun B, Xiao Ye J, Chen G, et al. Protective effects of Amygdalus mongolica on rats with renal fibrosis based on serum metabolomics. J Ethnopharmacol. 2020;257:11258.

Tables

Table 1 Thirty-eight differentially expressed metabolites selected and identified between the MOD and CON groups.

NO.	Matabolites	M/S	Retention time	MS1hmdbID	VIP[a]	Regulated (M/C)	Regulated (B/M)	Regulated (A/M)
	Positive ion mode							
1	4E,15Z-BilirubinIXa	585	454	HMDB0000488	3.40	↑#		
2	Ornithine	133	45	HMDB0000214	3.23	↑#		
3	Succinyladenosine	384	129	HMDB0000912	3.33	↑#	↓*	↓*
4	Diketogulonic acid	215	65	HMDB0005971	2.29	↑#	↓*	
5	Tetracosahexaenoic acid	357	187	HMDB0002007	2.40	↑#		
6	Tauroursodeoxycholic acid	544	158	HMDB0000874	2.40	↑#		
7	o-Tyrosine	182	124	HMDB0006050	2.04	↑#	↓*	
8	N-Acetylarylamine	136	68	HMDB0001250	2.19	↑#		
9	4-Hydroxy-4-(3-pyridyl)-butanoic acid	182	68	HMDB0001119	2.19	↑#		
10	Tetradecanoylcarnitine	372	187	HMDB0005066	2.34	↑#		
11	dIMP	371	171	HMDB0006555	2.34	↓#	↑*	↑*
12	5,6-Dihydrouridine	247	163	HMDB0000497	2.65	↓#		↑*
13	4-Imidazolone-5-propionic acid	157	171	HMDB0001014	2.70	↓#	↑*	↑*
14	3'-O-Methylguanosine	315	177	HMDB0006038	2.38	↓#		
15	12a-Hydroxy-3-oxocholadienic acid	387	182	HMDB0000385	2.40	↓#		
16	Phenylalanyl-Threonine	267	0.170	HMDB0029005	3.37	↓#	↑*	↑*
17	Methionyl-Threonine	268	170	HMDB0028983	3.42	↓#	↑*	↑*
18	Homoanserine	255	209	HMDB0005767	3.37	↓#	↑*	↑*
19	3-Hydroxypicolinic acid	157	143	HMDB0013188	3.98	↓#	↑*	↑*
20	Hydroxyprolyl-Isoleucine	245	170	HMDB0028866	3.65	↓#	↑*	↑*
21	9'-Carboxy-alpha-chromanol	391	174	HMDB0012866	3.02	↓#		
22	Acetyl-N-formyl-5-methoxykynurenamine	265	170	HMDB0004259	3.88	↓#	↑*	↑*
	Negative ion mode							
23	Cysteinyl-Proline	217	143	HMDB0028783	3.01	↑#		
24	Nicotinicacid mononucleotide	336	91	HMDB0001132	2.92	↑#	↓*	↓*
25	L-beta-aspartyl-L-serine	236	150	HMDB0011168	2.78	↑#	↓*	
26	Inodxyl glucuronide	325	290	HMDB0010319	2.43	↑#		↓*
27	S-Adenosylmethioninamine	.354	148	HMDB0000988	2.30	↑#		

28	Neuraminic acid	283	149	HMDB0000830	2.56	↑#	↓*	↓*
29	Methionyl-Tryptophan	351	108	HMDB0028984	2.19	↑#		
30	Dopamine glucuronide	345	108	HMDB0010329	2.05	↑#		↓*
31	Tetragastrin	333	93	HMDB0005775	2.30	↓#		
32	N-Acetyl-D-Glucosamine 6-Phosphate	317	145	HMDB0001062	2.11	↓#		
33	SR 49498	505	209	HMDB0013845	2.14	↓#	↑*	
34	APGPR Enterostatin	533	186	HMDB0006117	2.08	↓#		
35	Aminoparathion	277	143	HMDB0001504	2.66	↓#	↑*	↑*
36	Propionylcholine	159	163	HMDB0013305	3.17	↓#	↑*	↑*
37	Tyrosyl-Tyrosine	360	209	HMDB0029117	2.33	↓#		↑*
38	Tetrahydrofolyl-[Glu](2)	573	143	HMDB0006825	4.27	↓#	↑*	↑*

Note: a,VIP values were obtained from PLS-DA model. # compared with the CON group; * compared with the MOD group. ↑, content increased; ↓, content decreased.M, MOD. A, AMY. B, BUT.

Figures

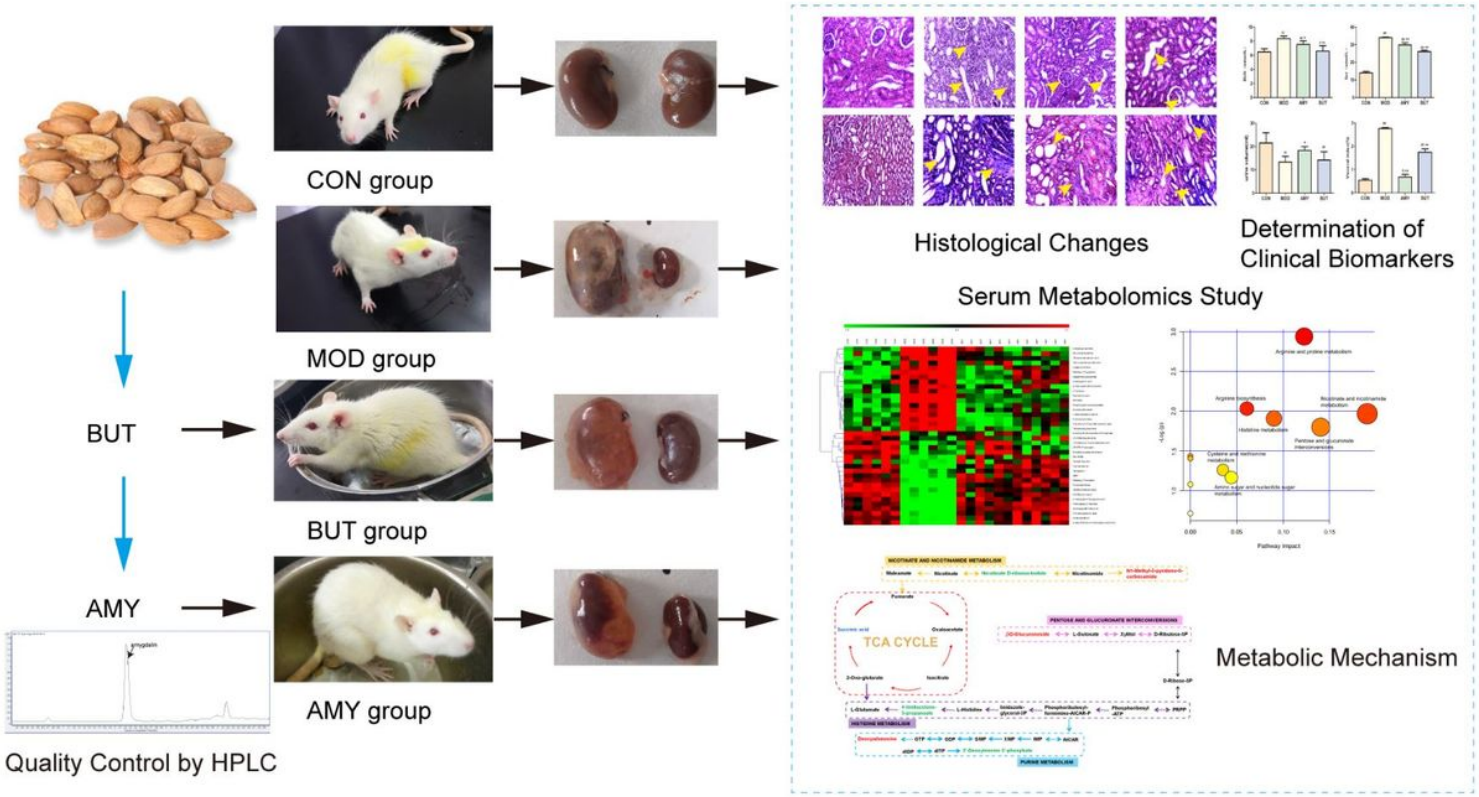

Figure 1

Scheme of the study.

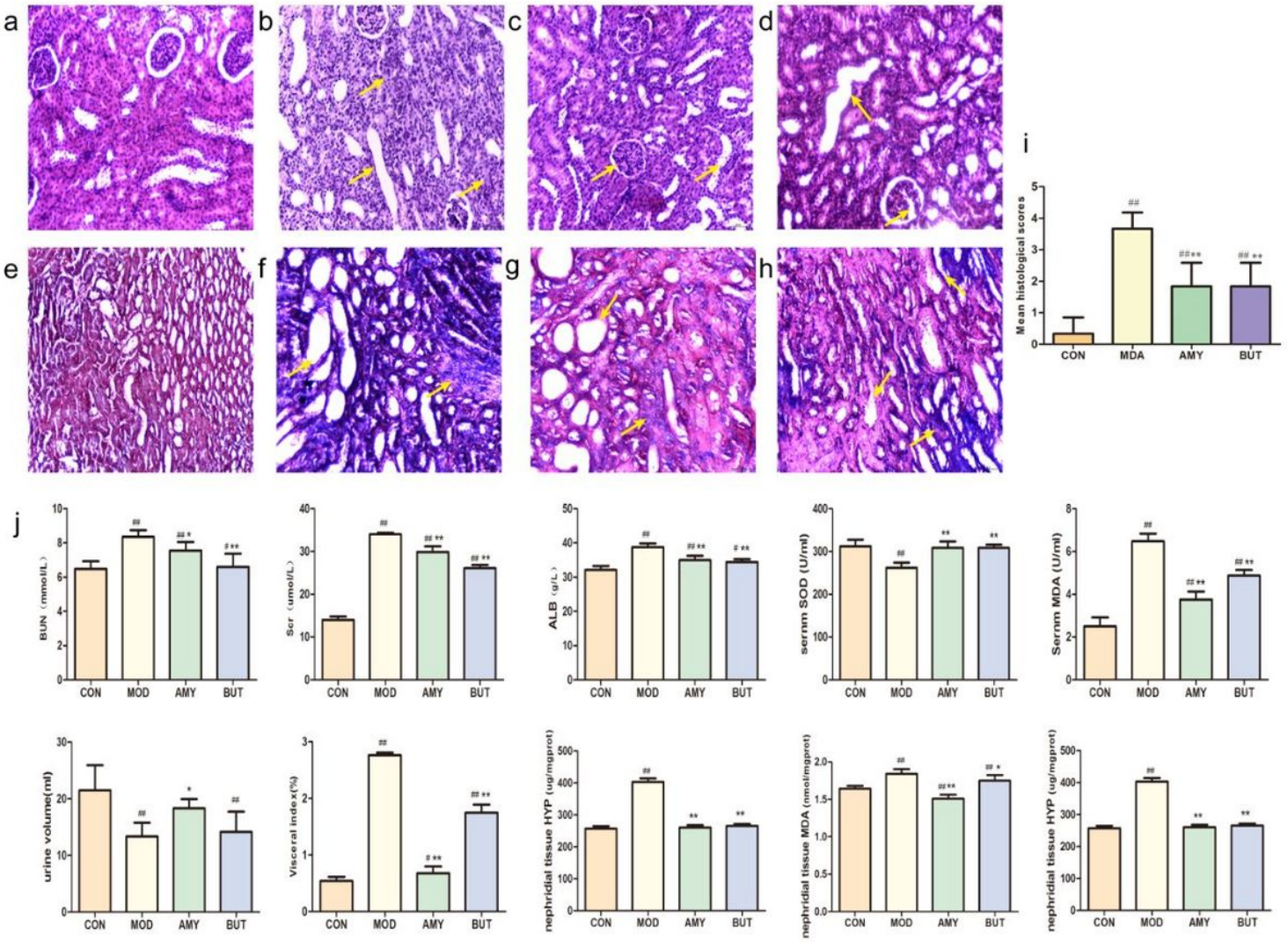

Figure 2

Pathological renal sections and determination of biochemical indicators in the CON, MOD, AMY, and BUT. (a-h) Renal tissues were stained using H&E (×200) and Masson staining (×400). Arrows indicate the lesion site. (i) The histopathological score results. (j) Determination of BUN, Scr, ALB, MDA, SOD, and HYP. All values are presented as the mean ± SD. Statistical significance was calculated with ANOVA. *P < 0.05 and **P < 0.01 compared to the MOD group. #P < 0.05 and ##P < 0.01 compared to the CON group. The degree of severity was assigned the following scores according to the extent of injured cortex areas: 0, normal cortex; 1, < 25% of the cortex area was injured; 2, 26 to 50% of the cortex area was injured; 3, 51 to 75% of the cortex area was injured; and 4, > 75% of the cortex area was injured.

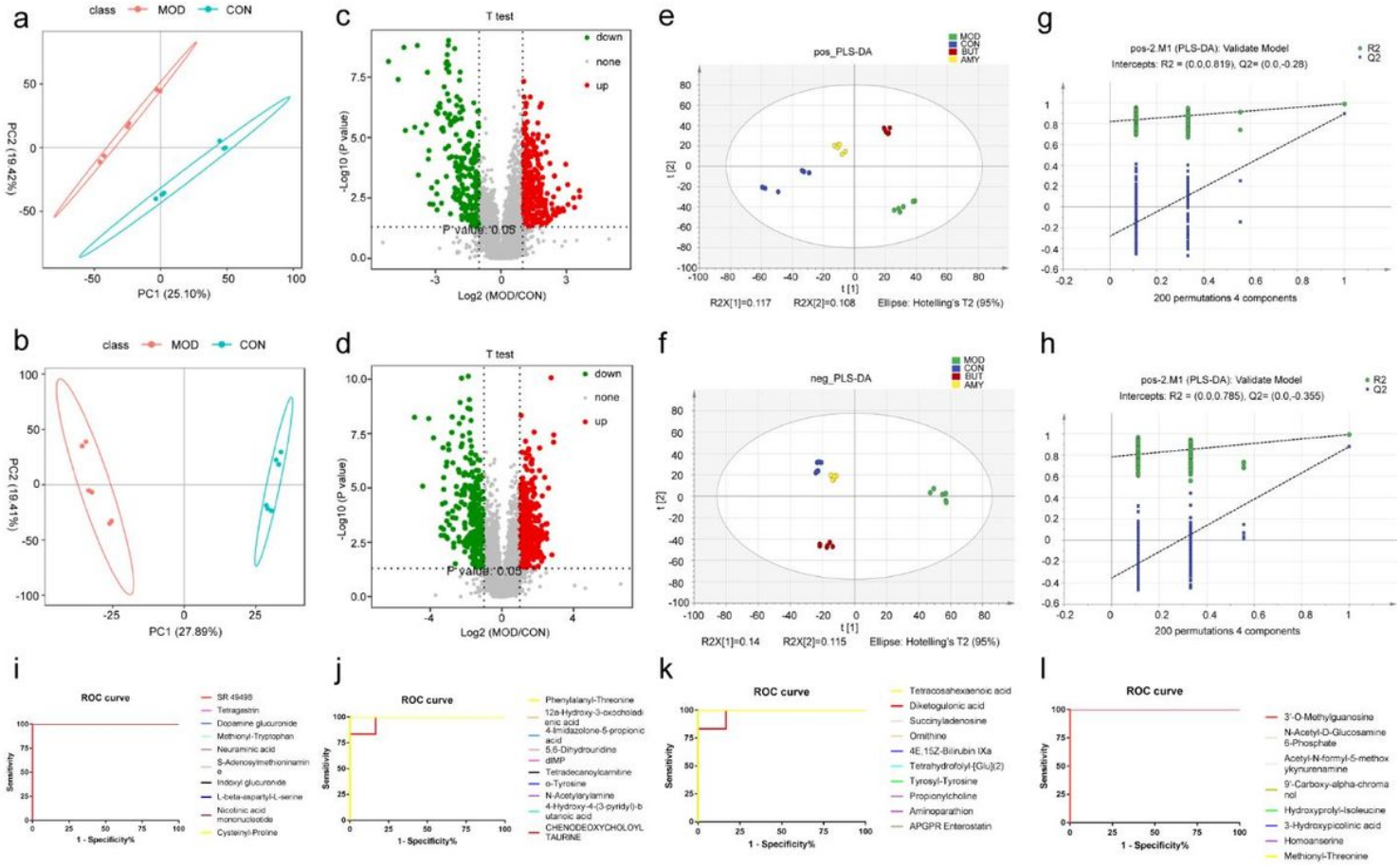

Figure 3

PCA and PLS-DA score plots of the serum samples from each group and ROC curve. (a, b) PCA score plots of the CON and MOD groups in positive and negative mode, respectively. (c, d) V-plot of the CON and MOD groups in positive and negative mode. (e, f) PLS-DA score plots in positive and negative mode, respectively. (g, h) Verification of the PLS-DA models by class permutation tests in positive and negative mode, respectively. (i-l) ROC analysis of 38 potential biomarkers.

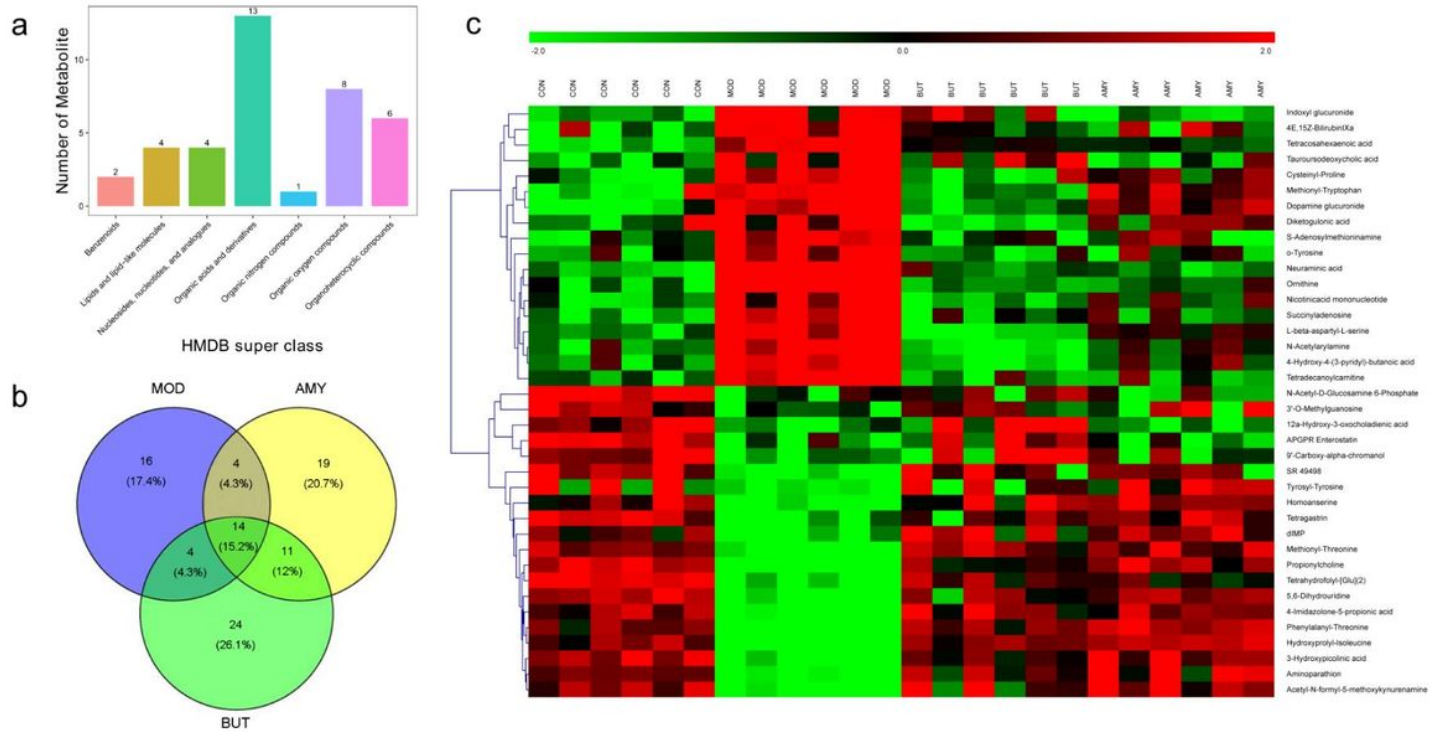

Figure 4

Analysis of the differentially expressed metabolites. (a) The classification of the 38 identified potential biomarkers in serum samples. (b) Venn diagram of all impacted variables (VIP > 2, P < 0.05) in the comparisons of the AMY and BUT with the MOD. (c) Heat map of the differential abundance of metabolites in each group. Rows, samples; columns, metabolites. The degree of color saturation indicates the metabolite expression value, with blue representing the lowest expression and red representing the highest expression.

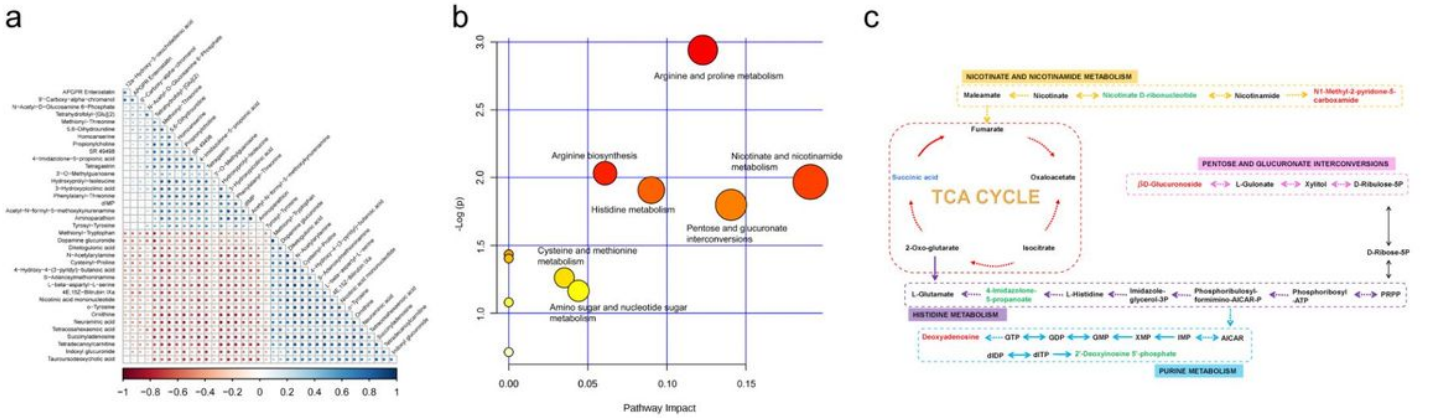

Figure 5

Analysis of potential biomarkers and related metabolic pathways. (a) Pearson rank correlation analysis between 38 potential biomarkers. The red and blue color saturation represents the positive and negative correlation coefficients, respectively, between the markers. (b) Summary of the altered metabolism pathways determined with MetPA. The size and color of each circle are based on pathway impact value and P-value, respectively. (c) Network of the identified key biomarkers and pathways of BUT and AMY treatment according to the KEGG pathway database. The metabolites colored green represent common metabolites in "BUT" and "AMY".

Supplementary Files

This is a list of supplementary files associated with this preprint. Click to download.

- TableS2.docx
- TableS1.docx
- supplenmentinformation1.docx
- TableS3.docx